Structural Safety, 12 (1993) 35–57
Elsevier

Comparison of analytical counting methods for Gaussian processes *

V. Bouyssy

Technical University of Munich, München, Germany

S.M. Naboishikov

Technical University of Vinniza, Vinniza, Ukraine

R. Rackwitz

Technical University of Munich, Lehrstuhl für Massivbau, Arcisstr. 21, D-8000 München 2, Germany

Abstract. For structural components under random loading, realistic fatigue life predictions require a damage accumulation law together with a cycle counting method. If the classical, linear and memory-less summation rule according to Palmgren/Miner is adopted and the underlying stress process is ergodic substantial simplifications can be reached. From experiments and certain theoretical considerations, so-called rainflow range or local range counting appears most appropriate. Even if the underlying is a Gaussian process, easy analytical solutions are at most available for special types of processes. Therefore, counting usually must be done numerically at observed or artificial stress histories which is extremely time consuming. But a number of approximations exist. Several of them are reviewed and tested against simulations for a variety of bandwidths and shapes of stress spectra. While most of the prediction equations overestimate the moments of the two selected types of ranges, the equation provided by Dirlik is shown to have the best fit with respect to the simulated rainflow ranges. Naboishikov's formula proves to be the most accurate predictor for local ranges whenever the irregularity factor α is larger than 0.6.

Key words: fatigue accumulation; local ranges; Gaussian process; cycle counting methods.

1. Introduction

The assessment of fatigue damage under random loading requires essentially two concepts, one for the accumulation of damage and one for the counting of the damage relevant cycles. At

* Discussion is open until October 1993 (please submit your discussion paper to the Editor, Ross B. Corotis).

present, fatigue damage accumulation is mostly described by using the Palmgren–Miner [1,2] rule for both initiation and propagation of a crack. This linear law can formally be expressed as

$$\frac{\mathrm{d}D}{\mathrm{d}n} = \frac{1}{K} S^m \tag{1}$$

where K and m are deterministic material constants and S denotes some function of the stress process. In most cases S is a function of the stress range and, possibly, the maximum stress or, equivalently, the range mean. Integration of eqn. (1) yields

$$\int_0^{D(N)} \mathrm{d}D = D(N) = \frac{1}{K}\int_0^N S^m \,\mathrm{d}n \approx \frac{1}{K}\sum_{i=1}^{N} S_i^m \sim \frac{1}{K} NE[S^m] \tag{2}$$

where N is the number of cycles up to the accumulated damage $D(N)$. The stress ranges are assumed to form an ergodic sequence, which allows to replace the time integration by N-times the expected value of S^m. The ergodicity assumption also implies that the right-hand side of this equation is linear in N and that $E[S^m]$ becomes constant for sufficiently large N. Thus, no variability consideration for the damage indicator $NE[S^m]$ is needed.

Even if the underlying process is supposed to be Gaussian, no simple definition of the quantity S exists. Moreover, no general analytical method is available to estimate the damage relevant number N of cycles and especially the damage indicator $E[S^m]$ from the stress time-history. But several approximate counting methods based on different concepts exist (see Madsen et al. [3] for a review). At present, the "rainflow" counting method is considered to best reflect the mechanics of fatigue damage accumulation for metals whenever substantial non-local plastic strains arise. It provides the rainflow range and its associated moments. The stress cycles are defined as a series of closed hysteresis loops in the stress-strain response. Fatigue damage is related to the area enclosed by these loops. Empirically, the material constant m is found to be between 2 and 8. The rainflow range moments might also be the most accurate local damage indicators for crack propagation in metals whenever the crack advance in a cycle can be related to the work done in the crack tip plastic zone. As shown, for example, by Paris [4] and Rice [5], the crack growth rate is then proportional to the fourth power of the stress intensity factor range. However, the crack growth rate appears to be only proportional to the second power of the stress intensity factor range (see, for example, Weertman [6]) for intrinsically ductile metals. By considering the associated mechanism of crack propagation, the rainflow range moments appear in this case less suitable than the moments of the local range. Also, the rainflow range moments do not necessarily appear to be the most accurate local damage indicators for the propagation of cracks in relatively brittle materials and for crack initiation in ductile materials. In the last case, the local stress intensity maximum together with the associated local range may be considered as the best damage indicator. In summary, the suitability of the rainflow range or of the local range strongly depends on the specific characteristics of the material and on its damage state (Manson [7], Short/Hoeppner [8]). The use of either quantity must be justified on empirical grounds. Both methods lead to the same result for pure narrow band process. For broad band processes rainflow ranges lead to an upper bound for the accumulated damage while local ranges lead to a lower bound. Therefore, both types of damage indicators will be studied in the following.

Analytical results for $NE[S^m]$ are available for the special case of an ideally narrow band stationary Gaussian process, only. A proposal to analytically predict the rainflow ranges was made by Rychlik [9,10]. Unfortunately, this approach is rather time consuming and is thus not yet practical. Most frequently, the rainflow ranges are determined by first simulating the stress process time-history and then by analyzing this process statistically. Simulation and statistical analysis can be extremely laborious. A number of approximations were therefore proposed. The purpose of the following study is to review some of the suggested approximations and to test them against simulated rainflow and local range countings. A critical comparison of their performance using several load spectra is presented and some recommendations for practical applications are given.

2. Review of prediction equations

For convenience of notation we assume that the underlying Gaussian process $X(t)$ has zero mean and unit variance. If the standard deviation of the original process is σ, the damage indicator for this process is simply $N\sigma^m E[S_X^m]$ with $NE[S_X^m]$ the damage indicator for the standardized process. In the following, reference to the process $X(t)$ will be omitted. The process $X(t)$ can to some extent be characterized by a few parameters such as the sequence of spectral moments

$$m_i = \int_0^\infty \omega^i G(\omega)\,\mathrm{d}\omega$$

where $G(\omega)$ is the one-sided power spectral density. In general, only the first few spectral moments can be determined. Higher moments imply increasing requirements on the differentiability of the process and may not exist. The following bandwidth parameters can be defined.

$$\delta = \frac{m_1}{\sqrt{(m_0 m_2)}} \tag{4}$$

$$\alpha = \frac{m_2}{\sqrt{(m_0 m_4)}} \tag{5}$$

$$\epsilon^2 = 1 - \alpha^2 \tag{6}$$

with their limit values given in Table 1.

The earliest approximation for $NE[S^m]$ is due to Miles [11] and is valid for pure narrow band stationary Gaussian processes (see below). If this formula is applied to processes with larger bandwidth, the damage can be considerably overestimated, especially for larger m. Many of the more recent approximations set out from this result by introducing additional parameters

TABLE 1

Limit values of bandwith parameters α, δ and ϵ

	α	δ	ϵ
Ideally narrow band process	1.0	1.0	0.0
Ideally broad band process	0.0	0.0	1.0

describing the correlation structure of the underlying process. Those parameters are either derived from theoretical considerations or are determined empirically.

2.1. Narrow-band processes

The local peaks Y^+ or Y^- of a pure narrow band process are Rayleigh distributed. Adjacent peaks are supposed to be perfectly correlated, which means that all positive peaks are matched with corresponding troughs of the same magnitude. The stress range then is Rayleigh distributed, too, and the damage indicator is calculated as (Miles [11])

$$NE[S^m] = N(2\sqrt{2})^m \Gamma\left(1+\frac{m}{2}\right) \tag{7}$$

The number N of stress cycles in a given time interval $[0, t]$ is equal to the expected number of local maxima in $[0, t]$ given by

$$N = t\sqrt{\frac{m_4}{m_2}}\,\frac{1}{2\pi} \tag{8}$$

which in this particular case also corresponds to the expected number of positive zero crossings in $[0, t]$

$$N = t\sqrt{\frac{m_2}{m_0}}\,\frac{1}{2\pi} \tag{9}$$

Yang [12] generalized Miles' result to not perfectly correlated local peaks. The local range is derived from the bivariate Rayleigh distribution. The equation providing the m-th moment involves the hypergeometric function. The correlation coefficient between adjacent peaks or the local minimum and its consecutive local maximum must be known. Yang [12] provided an approximation for this correlation coefficient for narrow band processes. In particular, the expected value of the m-th power of the stress range is derived as

$$E[S^m] = E\left[(|Y^-|+Y^+)^m\right] = E\left[\sum_{i=0}^{m}\binom{m}{i}|Y^-|^{m-i}(Y^+)^i\right] = \sum_{i=0}^{m}\binom{m}{i}E\left[|Y^-|^{m-i}(Y^+)^i\right]$$

with

$$E\left[|Y^-|^{m-i}(Y^+)^i\right] = E\left[|Y^-|^a(Y^+)^b\right] = (\sqrt{2})^{a+b}\Gamma\left(1+\frac{a}{2}\right)\Gamma\left(1+\frac{b}{2}\right){}_2F_1\left(-\frac{a}{2}, -\frac{b}{2}; 1; k^2\right) \tag{10}$$

where ${}_2F_1(\ )$ denotes the hypergeometric function and k is a correlation parameter. As k tends to 1, the hypergeometric function converges to

$$F_1\left(-\frac{a}{2}, -\frac{b}{2}; 1; 1\right) = \Gamma\left(1+\frac{a+b}{2}\right)\Big/\left(\Gamma\left(1+\frac{a}{2}\right)\Gamma\left(1+\frac{b}{2}\right)\right)$$

and Miles' result is recovered.

Another similar derivation is based on the definition of a so-called double envelope process (Krenk [13]). The corresponding damage indicator is

$$E[S^m] = \alpha^{m-1}(2\sqrt{2})^m \Gamma\left(1+\frac{m}{2}\right) \tag{11}$$

The correction factor to Miles' result $\lambda_k = \alpha^{m-1}$ tends to 1 as α approaches 1. The concept of a double envelope implies that the resulting predictions are only accurate for nearly narrow band processes. For the particular case of unimodal load spectra, Winterstein/Cornell [14] derived another empirical correction factor with a wider range of applicability by using a different envelope concept. It is not presented herein.

2.2. Broad band processes

Various attempts have been made in order to extend these analytical results to broad band processes with moderate success. The only exact analytical solution is for the mean of the stress range derived first by Rice/Beer [15].

$$E[S] = \sqrt{2}\,\pi\alpha \tag{12}$$

Jiao/Moan [16] extended the approach for narrow band processes to the important case of a process with two well separated spectral peaks. The damage correction factor is

$$\lambda_{\mathrm{J.M}} = \frac{\nu_p}{\nu_y}\left[\lambda_1^{2+m/2}\left[1-\sqrt{\frac{\lambda_2}{\lambda_1}}\right] + m\sqrt{\pi\lambda_1\lambda_2}\,\frac{\Gamma\left(\frac{m}{2}+\frac{1}{2}\right)}{\Gamma\left(\frac{m}{2}+1\right)}\right] + \frac{\nu_2}{\nu_y}\lambda_2^{m/2} \tag{13}$$

with

$$\nu_p = \lambda_1\nu_1\left[1+\frac{\lambda_2}{\lambda_1}\left(\frac{\nu_2}{\nu_1}\delta_2\right)^2\right]^{1/2}, \quad \nu_y = \left(\lambda_1\nu_1^2+\lambda_2\nu_2^2\right)^{1/2}, \quad \lambda_1 = \frac{m_{0,1}}{m_{0,1}+m_{0,2}}, \quad \lambda_2 = \frac{m_{0,2}}{m_{0,1}+{}_{0,2}},$$

$$\nu_1 = (m_{2,1}/m_{0,1})^{1/2}, \qquad \nu_2 = (m_{2,2}/m_{0,2})^{1/2}, \qquad \delta_2 = \left[1-\frac{m_{1,2}^2}{m_{0,2}/m_{2,2}}\right]^{1/2},$$

where $(m_{i,j},\ i=0, 2,\ j=1, 2)$ are the spectral moments in the two spectral bands. In the particular case of a bimodal white noise spectrum, these moments are

$$m_{0,1} = C_1(\omega_2-\omega_1), \qquad m_{0,2} = C_2(\omega_4-\omega_3),$$
$$m_{1,1} = \tfrac{1}{2}C_1(\omega_2^2-\omega_1^2), \qquad m_{1,2} = \tfrac{1}{2}C_2(\omega_4^2-\omega_3^2),$$
$$m_{2,1} = \tfrac{1}{3}C_1(\omega_2^3-\omega_1^3), \qquad m_{2,2} = \tfrac{1}{3}C_2(\omega_4^3-\omega_3^3),$$

where $\omega_1 \leqslant \omega \leqslant \omega_2$ and $\omega_3 \leqslant \omega \leqslant \omega_4$ are the two representative frequency bands.

Other damage indicator formulae are based on the statistical study of local extrema of a stationary Gaussian process. Assuming that this process is nearly narrow band, its local extrema are nearly Rayleigh distributed and symmetric. Moreover, if local maxima and minima are supposed to be matched in pairs of same magnitude, the damage relevant stress range is exactly twice the amplitude of local maxima. A first result based on local peaks has been derived by Hancock/Gall [17] by neglecting the broad band term in the probability distribution of local maxima (see eqn. (16) below). Their result is

$$E[S^m] = \alpha(2\sqrt{2})^m \Gamma\left(1+\frac{m}{2}\right) \tag{14}$$

The correction factor to eqn. (7) is then

$$\lambda_H = \alpha \tag{15}$$

It differs from the double envelope results in eqn. (11) by the exponent of α. Among others Tunna [18] followed a similar approach also accounting for different slopes in the S–N curve.

Using earlier results from Chaudhury/Dover (1982) and Hancock/Gall [17], Kam/Dover [19] introduced an improvement based on the exact probability distribution of local maxima whose density is

$$p(y^+) = \frac{\epsilon}{\sqrt{(2\pi)}} \exp\left[-\frac{1}{2}\left(\frac{y^+}{\epsilon}\right)^2\right] + \alpha y^+ \exp\left[-\tfrac{1}{2}(y^+)^2\right]\Phi\left(\frac{\alpha}{\epsilon} y^+\right) \tag{16}$$

This density is the sum of a Gaussian density and a term which tends to the Rayleigh density for large y^+. The expectation of twice the amplitude of local maxima is taken. The following approximate damage indicator is obtained

$$E[S^m] = (2\sqrt{2})^m \left[\frac{\epsilon^{m+2}}{2\sqrt{\pi}}\Gamma\left(\frac{1+m}{2}\right) + \frac{1+\mathrm{erf}(\alpha, m)}{2}\alpha\Gamma\left(1+\frac{m}{2}\right)\right] \tag{17}$$

where erf(α, m) is the error function (Kam/Dover [19]). The expectation in eqn. (17) can also be taken analytically yielding (Abdo/Rackwitz [20])

$$E[S^m] = (2\sqrt{2})^m \left\{\frac{\epsilon^{m+2}}{2\sqrt{\pi}}\Gamma\left(\frac{1+m}{2}\right) + \alpha\Gamma\left(1+\frac{m}{2}\right) T_\nu\left(\frac{\alpha}{\epsilon}\sqrt{\nu}\right)\right\} \tag{18}$$

where $T_\nu(\cdot)$ is Student's central t-distribution with $\nu = m + 2$ degrees of freedom. Furthermore, Abdo/Rackwitz [20] argued that the number of stress cycles should only correspond to the number of positive local maxima since negative local maxima do not contribute to damage. Therefore, these local maxima and the associated ranges should be neglected. The mean number of positive local maxima of S exceeding u in the time interval $[0, t]$ is given by

$$E[M_u^+(t)] = \frac{t}{2\pi}\left\{\left(\frac{m_4}{m_2}\right)^{1/2}\left(1 - \Phi\left(+u\left(\frac{m_4}{D}\right)^{1/2}\right)\right) + \sqrt{2\pi m_2}\,\phi(u)\Phi\left(+\frac{u m_2}{D^{1/2}}\right)\right\} \tag{19}$$

where $D = m_4 - m_2^2$ (Leadbetter et al. [21]). For a standardized process, the value $u = 0$ is taken and it follows that the total fatigue damage is

$$KD(N) = E[S^m]\,E[M_u^+(t)] \tag{20}$$

While the derivations based on peaks implicitly assume that the damage relevant stress range can be taken twice the amplitude of local maxima and, thus, that the stress process is nearly narrow band, Naboishikov [22] explicitly determined the joint probability distribution of stress ranges S and their means Z. It can be proved that these quantities are uncorrelated and there are good reasons to assume that they are also independent. The range midpoints Z follow a normal distribution with zero mean and variance

$$\sigma_Z^2 = \tfrac{1}{2}\sigma_X^2(1+\alpha^2)(1+\rho) \tag{21}$$

where the parameter $\rho = \rho_{i,i+1}$ is the correlation coefficient between adjacent extrema. The probability density of stress ranges S is found as

$$p_S(s) = \frac{\epsilon^2\sigma_X^2 - \sigma_Z^2}{\sigma_X^2 - \sigma_Z^2}\frac{1}{\sqrt{2\pi}\sqrt{\epsilon^2\sigma_X^2 - \sigma_Z^2}}\exp\left[-\frac{1}{2}\left(\frac{s}{2\sqrt{\epsilon^2\sigma_X^2 - \sigma_Z^2}}\right)^2\right]$$
$$+ \frac{\alpha\sigma_X s}{2(\sigma_X^2 - \sigma_Z^2)^{3/2}}\exp\left[-\frac{1}{2}\left(\frac{s}{2\sqrt{\sigma_X^2 - \sigma_Z^2}}\right)^2\right]\left[\Phi\left(\frac{\alpha\sigma_X s}{2\sqrt{\sigma_X^2 - \sigma_Z^2}\sqrt{\epsilon^2\sigma_X^2 - \sigma_Z^2}}\right) - \frac{1}{2}\right] \tag{22}$$

A crude empirical approximation for the correlation coefficient is $\rho \approx 1 - 2\alpha$ (see below). It follows that the damage indicator is

$$E[S^m] = 2(2\sqrt{2})^m\left\{\sigma_1^m C_1\frac{1}{2\sqrt{\pi}}\Gamma\left[\frac{1+m}{2}\right] + \sigma_2^m a\Gamma\left[1+\frac{m}{2}\right]\left(T_\nu\left[\frac{a\sqrt{\nu}}{\sqrt{1-a^2}}\right] - \frac{1}{2}\right)\right\} \tag{23}$$

where

$$\sigma_1^2 = \epsilon^2\sigma_X^2 - \sigma_Z^2, \quad \sigma_2^2 = \sigma_X^2 - \sigma_Z^2, \quad C_1 = \sigma_1^2/\sigma_2^2, \quad C_2 = 1 - C_1, \quad a = \sqrt{C_2}, \quad \nu = m + 2$$

A number of investigators took a less theoretical approach. One of the earliest empirical formula is due to Wirsching [23,24]

$$E[S^m] = \lambda_W(2\sqrt{2})^m\Gamma\left(1+\frac{m}{2}\right) \tag{24}$$

where the correction factor λ to Miles' result (7) was empirically estimated as

$$\lambda_W = a + (1-a)(1-\epsilon)^b \tag{25}$$

with $a = 0.926 - 0.033\ m$ and $b = 1.587\ m - 2.323$. In this model, the correction parameter depends on the bandwidth parameter ϵ and the exponent m. The formula was calibrated at rainflow ranges obtained for simulated time-histories of several spectra occurring in the offshore industry. Another empirical correction factor was proposed by Madsen et al. [25]

$$\lambda_M = (0.93 + 0.07\,\alpha^5)^m \tag{26}$$

Recently, a few similar correction factors derived via simulation studies were suggested. Here we mention the proposal by Ortiz/Chen [26]

$$\lambda_{OC} = \frac{1}{\alpha}\left(\frac{m_2 m_b}{m_0 m_{2+b}}\right)^{1/2} \tag{27}$$

with a suggested value of $b = m/2$ and the simpler one by Larsen/Lutes [27]

$$\lambda_{LL} = m_{2/m}^{m/2} \tag{28}$$

In the foregoing empirical formulae (25)–(28), the stress ranges are implicitly assumed to be still approximately Rayleigh-distributed. In a part of the empirical studies this could not be confirmed by distribution tests. In line with these observations, Hancock/Gall [17] incorporate curve fitting parameters in a Weibull distribution of ranges and obtained the following correction factor (see also eqn. (15))

$$\lambda_H = \alpha \tag{29}$$

Moreover, other authors suggested to use a mixture of distributions. For example, Dirlik [28] proposed a combination of an exponential and two Rayleigh distributions for the rainflow ranges S with a probability density written as

$$p_S(s) = \frac{1}{2}\left\{\frac{D_1}{Q}\exp\left(-\frac{s}{2Q}\right) + \frac{sD_2}{2R^2}\exp\left(-\frac{1}{2}\left(\frac{s}{2R}\right)^2\right) + \frac{sD_3}{2}\exp\left(-\frac{1}{2}\left(\frac{s}{2}\right)^2\right)\right\} \tag{30}$$

where

$$D_1 = \frac{2(X_m - \alpha^2)}{1+\alpha^2}, \qquad D_2 = \frac{(1-\alpha-D_1+D_1^2)}{1-R}, \qquad D_3 = 1 - D_1 - D_2,$$

$$X_m = \frac{m_1}{m_0}\left(\frac{m_2}{m_4}\right)^{1/2}, \qquad Q = \frac{(\alpha - D_3 - RD_2)}{4D_1}, \qquad R = \frac{\alpha - X_m - D_1^2}{1-\alpha D_1 + D_1^2}$$

The damage indicator is then calculated as

$$E[S^m] = D_1\Gamma(1+m)(2Q)^m + \Gamma\left(1+\frac{m}{2}\right)(2\sqrt{2})^m(D_2R^m + D_3) \tag{31}$$

It should be noticed that this model uses four spectral moments. Zhao/Baker [29] used a similar concept for local ranges by assuming that the stress range probability distribution is a combination of one Weibull and one Rayleigh distributions. The probability density function is postulated as

$$p_S(s) = \tfrac{1}{2}\left\{wab\left(\frac{s}{2}\right)^{b-1}\exp\left(-a\left(\frac{s}{2}\right)^b\right) + (1-w)\frac{s}{2}\exp\left(-\frac{1}{2}\left(\frac{s}{2}\right)^2\right)\right\} \tag{32}$$

The mean of the stress range given in eqn. (12) is maintained and the weighting factor w is found as

$$w = \frac{1-\alpha}{1-\frac{\sqrt{2}}{\sqrt{\pi}}\Gamma\left(1+\frac{1}{b}\right)a^{-1/b}}$$

The Weibull parameters are determined from simulations on a wide range of spectra including the spectra used by Wirsching but are also supported by some theoretical arguments. Specifically, they are

$$a = 8 - 7\alpha \quad \text{and} \quad b = \begin{cases} 1.1 & \text{for } \alpha < 0.9 \\ 1.1 + 9(\alpha - 0.9) & \text{for } \alpha \geqslant 0.9 \end{cases}$$

The parameter b is close to one as in Dirlik's formula. The damage indicator is

$$E[S^m] = (2)^m\left(w\Gamma\left(1+\frac{m}{b}\right)a^{-m/b} + (1-w)(\sqrt{2})^m\Gamma\left(1+\frac{m}{2}\right)\right) \tag{33}$$

3. Numerical analysis

Although some further models have been proposed in the literature, the equations reviewed in Section 2 can be considered as being representative for the types of approaches. All

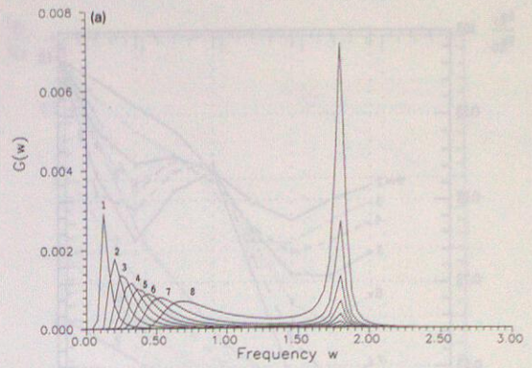

Fig. 1(a). Offshore spectra. 1—$T_d = 46.15$, $\alpha = 0.2$; 2—$T_d = 27.91$, $\alpha = 0.3$; 3—$T_d = 21.33$, $\alpha = 0.4$; 4—$T_d = 17.50$, $\alpha = 0.5$; 5–$T_d = 14.77$, $\alpha = 0.6$; 6—$T_d = 12.54$, $\alpha = 0.7$; 7—$T_d = 10.48$, $\alpha = 0.8$; 8—$T_d = 08.18$, $\alpha = 0.9$.

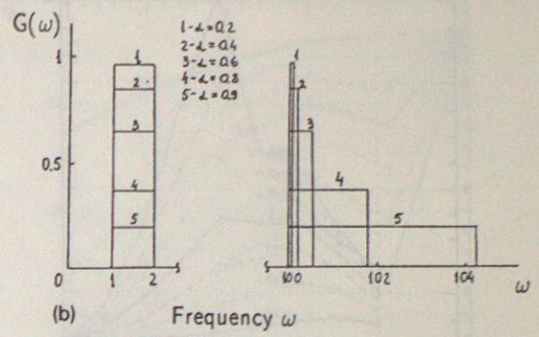

Fig. 1(b). Bimodal spectra.

approximations appear to be derived for special purposes. It must be expected that they fail outside of their range of calibration. Therefore, a numerical study has been designed covering a wide range of spectral shapes and bandwidths. Trajectories of Gaussian processes were simulated for several spectra. In order to avoid statistical uncertainties each trajectory contained at least 20000 local maxima. Analysis showed that statistical errors in the empirical damage indicators are then negligible even for exponents m as large as 8 and for arbitrary spectra. Four types of spectra are considered

a. offshore double-peak spectra (see Fig. 1(a));
b. bimodal band limited white noise (see Fig. 1b));
c. band limited white noise (see Fig. 1(c));
d. multimodal spectra (see Fig. 1(d)).

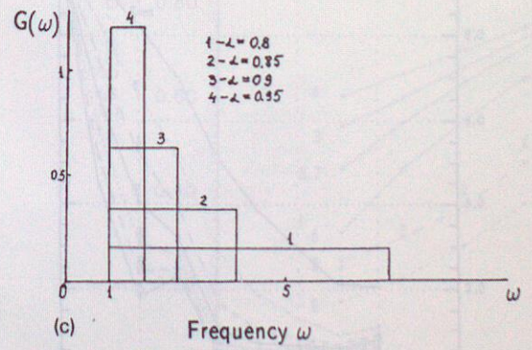

Fig. 1(c). Unimodal spectra.

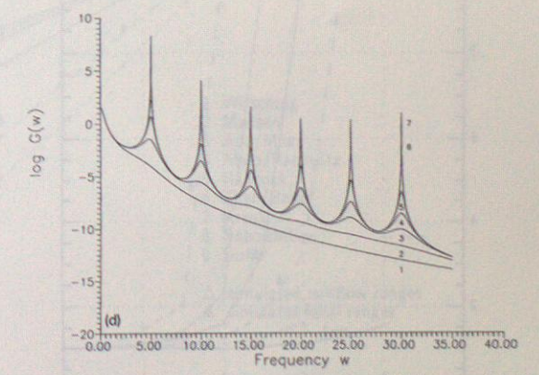

Fig. 1(d). Multimodal spectra. 1—$\beta = 0.500$, $\alpha = 0.139$; 2—$\beta = 0.135$, $\alpha = 0.195$; 3—$\beta = 0.045$, $\alpha = 0.300$; 4—$\beta = 0.20$, $\alpha = 0.395$; 5—$\beta = 0.007$, $\alpha = 0.505$; 6—$\beta = 0.001$, $\alpha = 0.604$; 7—$\beta = 0.0001$, $\alpha = 0.706$.

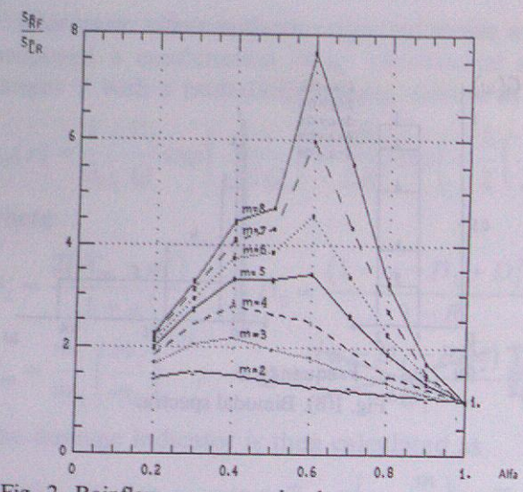

Fig. 2. Rainflow ranges vs. local ranges for offshore spectra.

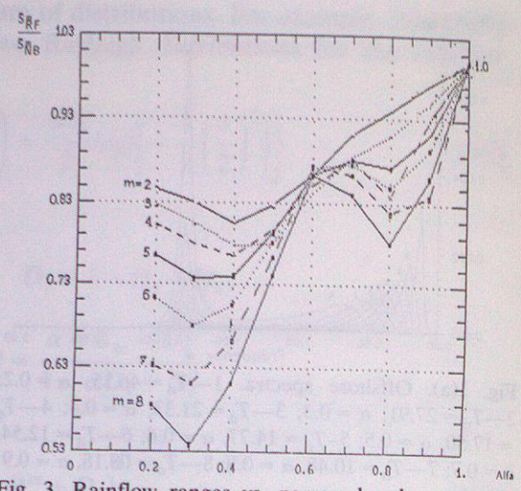

Fig. 3. Rainflow ranges vs. narrow band ranges for offshore spectra.

Their analytical forms and the simulation algorithm used are described in the Appendix. The multimodal spectrum is chosen because, for large α, it contains distinct spectral peaks which can be interpreted as belonging to a process possessing deterministic components at given frequencies. Such spectra are likely to occur, for example, in wind energy installations. The above spectra allow to cover a wide range of possible spectra which is necessary because the spectrum shape of a Gaussian process is not fully characterized by its first few spectral moments.

In Figs. 2 to 7, the relative behavior of the moments of the rainflow and local ranges are shown using the first three spectrum types. Two graphs were built for each type of stress

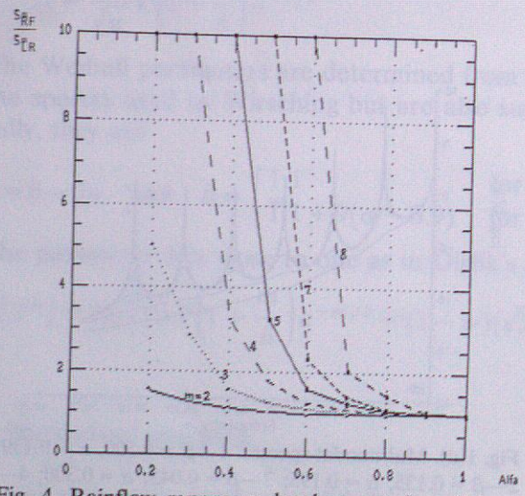

Fig. 4. Rainflow ranges vs. local ranges for offshore spectra.

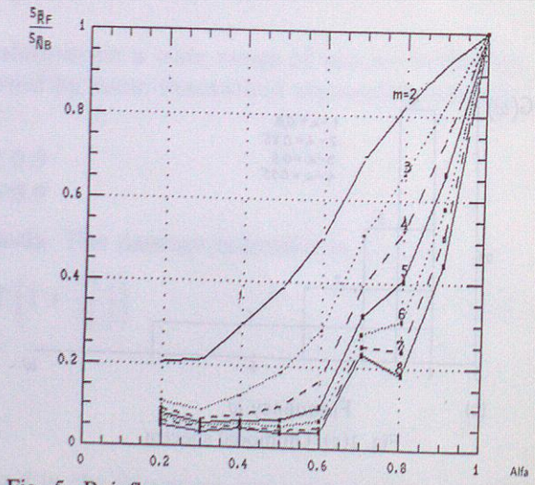

Fig. 5. Rainflow ranges vs. narrow band ranges for bimodal spectra.

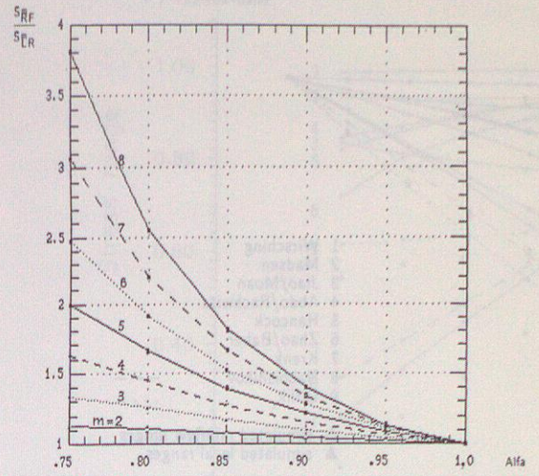

Fig. 6. Rainflow ranges vs. local ranges for unimodal spectra.

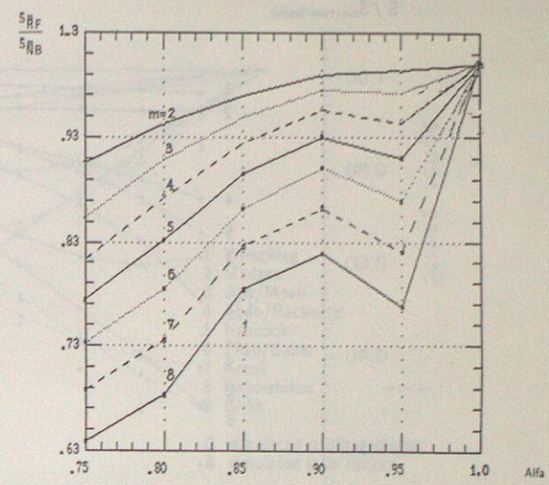

Fig. 7. Rainflow ranges vs. narrow band ranges for unimodal spectra.

spectrum. The ratios of the rainflow damage indicator to the local range and of the rainflow damage indicator to the Miles damage indicator are plotted as functions of the irregularity factor α. The large differences between the figures demonstrate that the local ranges cannot be used as a starting point for an analysis (or an approximation formula) whenever the rainflow ranges are considered as the best damage indicators from a mechanical point of view. The discrepancies become larger for higher values of m. They decrease as α tends to 1.

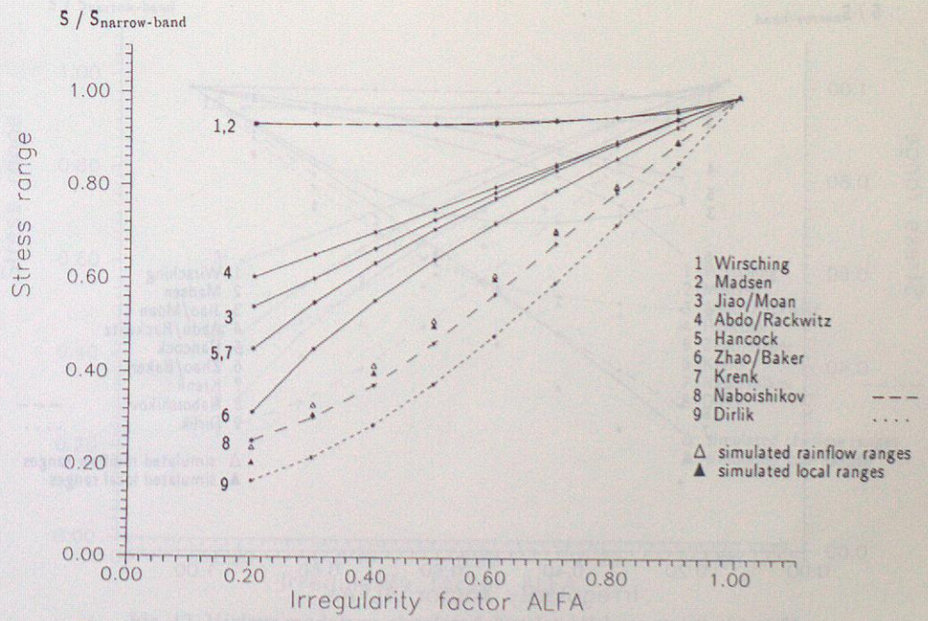

Fig. 8. Various models vs. simulated data for bimodal white noise spectra ($m = 2$).

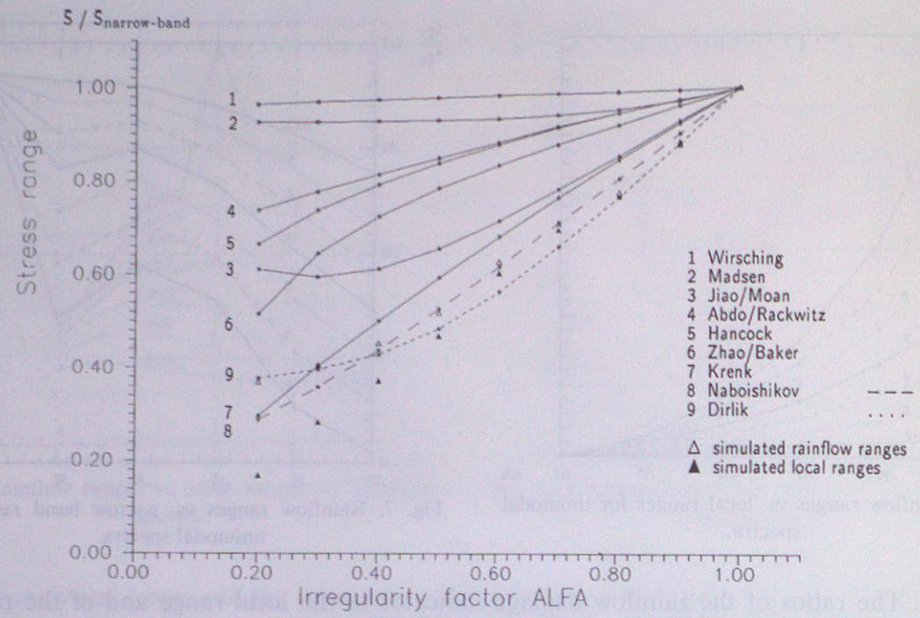

Fig. 9. Various models vs. simulated data for bimodal white noise spectra ($m = 4$).

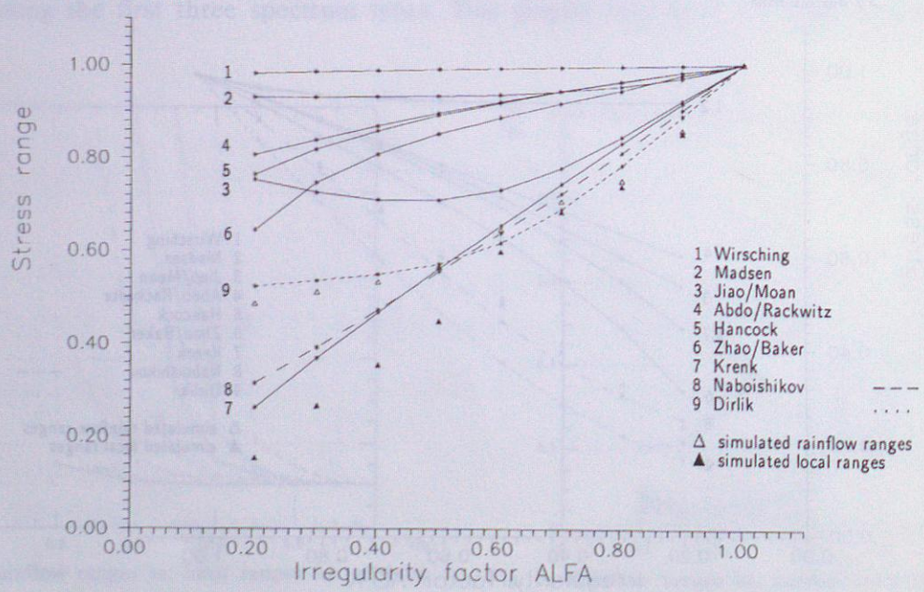

Fig. 10. Various models vs. simulated data for bimodal white noise spectra ($m = 6$).

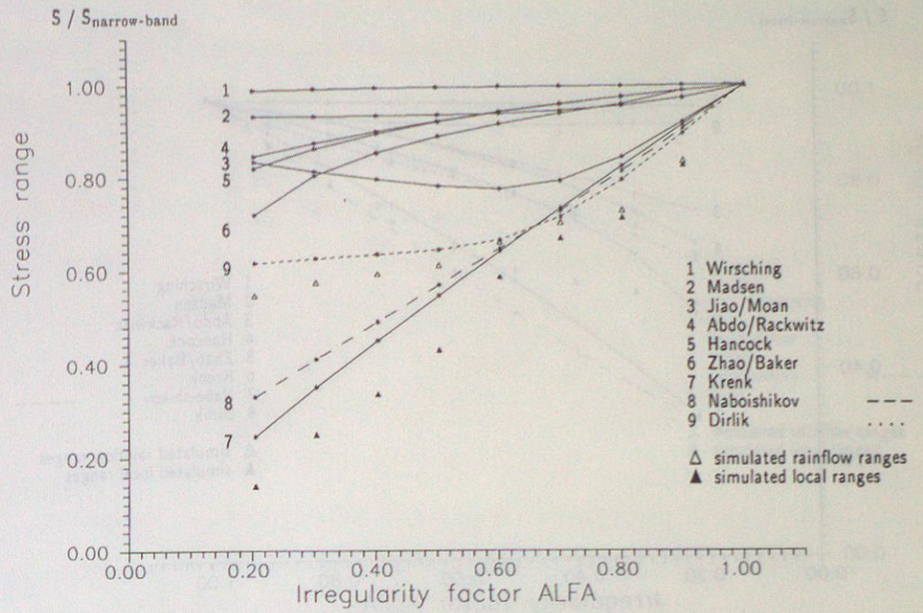

Fig. 11. Various models vs. simulated data for bimodal white noise spectra ($m = 8$).

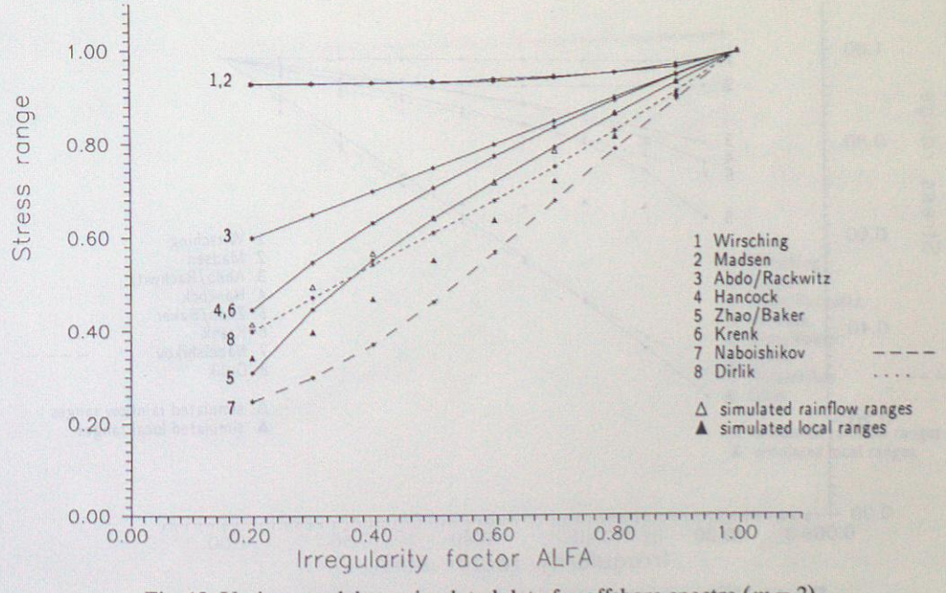

Fig. 12. Various models vs. simulated data for offshore spectra ($m = 2$).

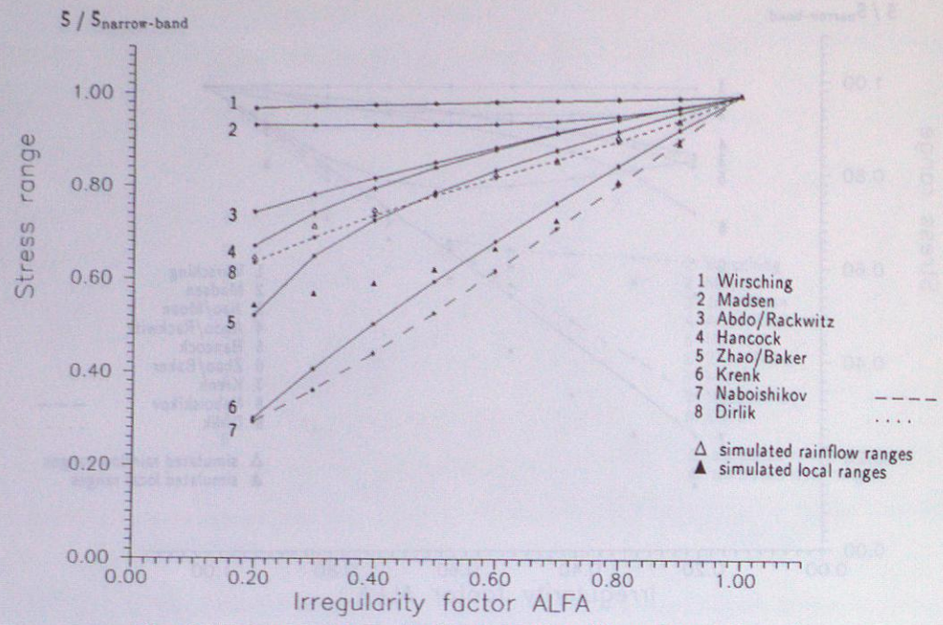

Fig. 13. Various models vs. simulated data for offshore spectra ($m = 4$).

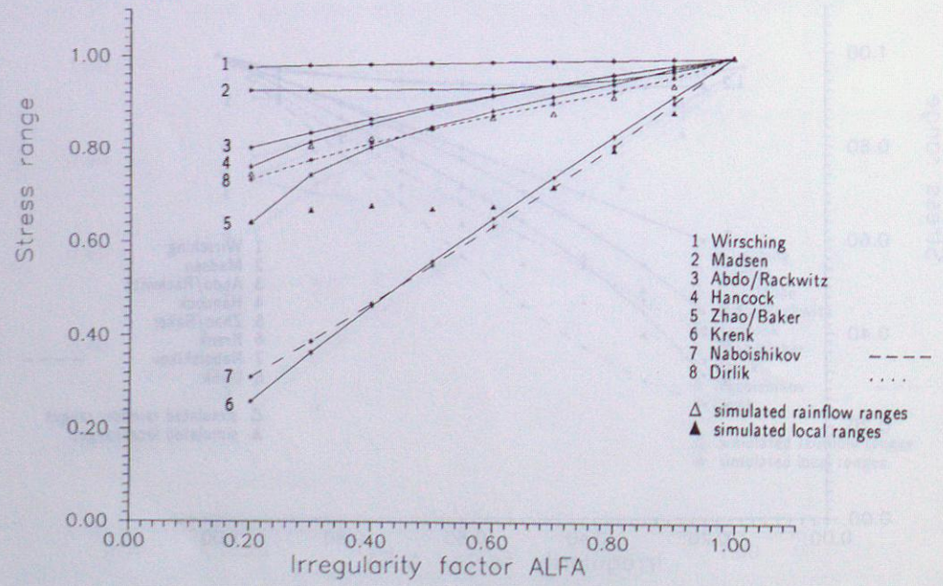

Fig. 14. Various models vs. simulated data for offshore spectra ($m = 6$).

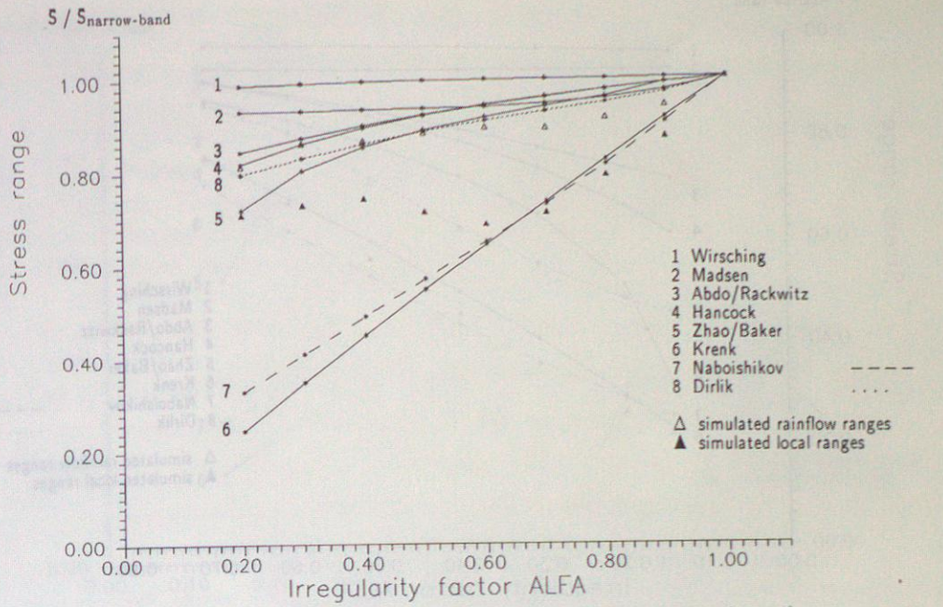

Fig. 15. Various models vs. simulated data for offshore spectra ($m = 8$).

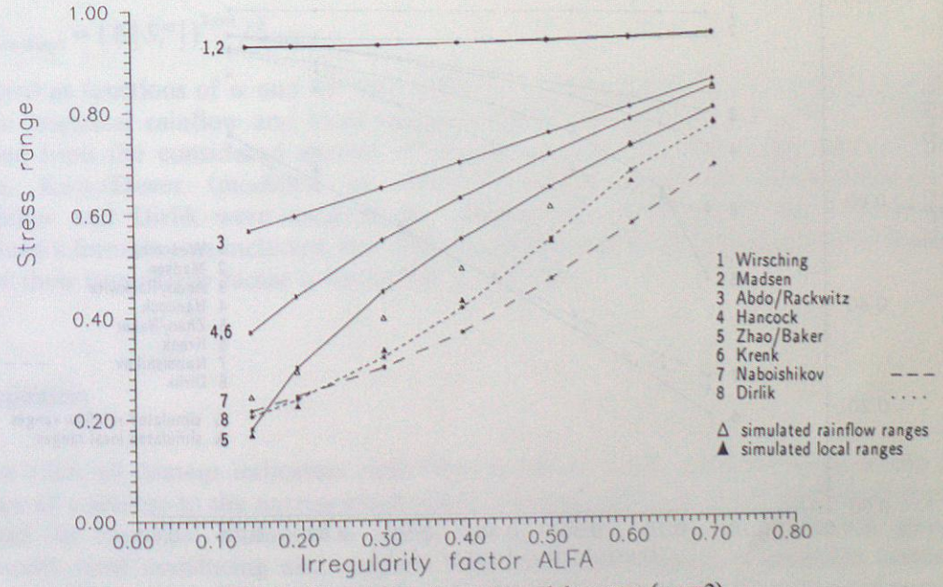

Fig. 16. Comparison for multimodal spectra ($m = 2$).

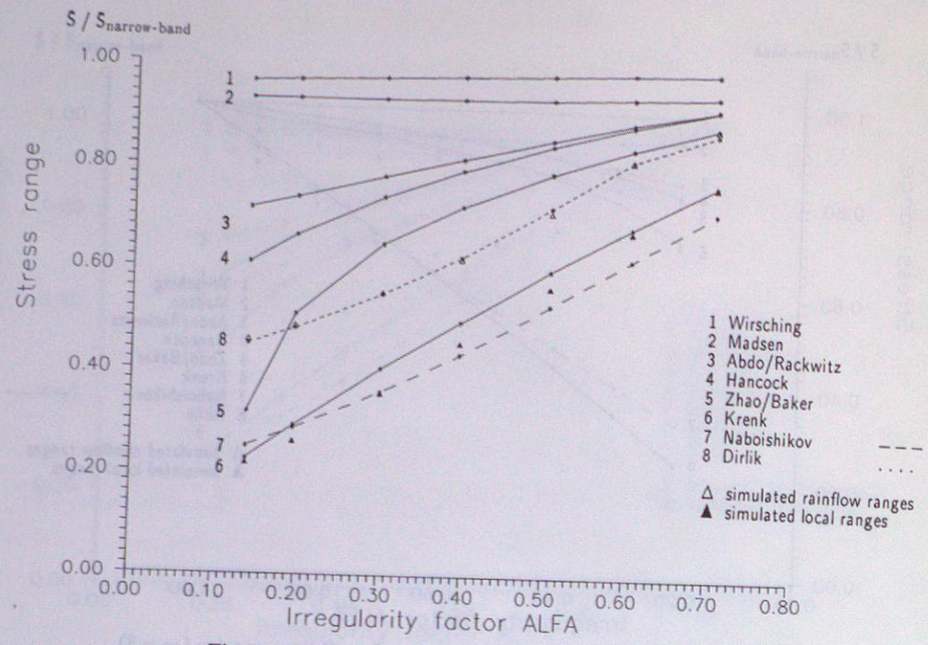

Fig. 17. Comparison for multimodal spectra ($m = 4$).

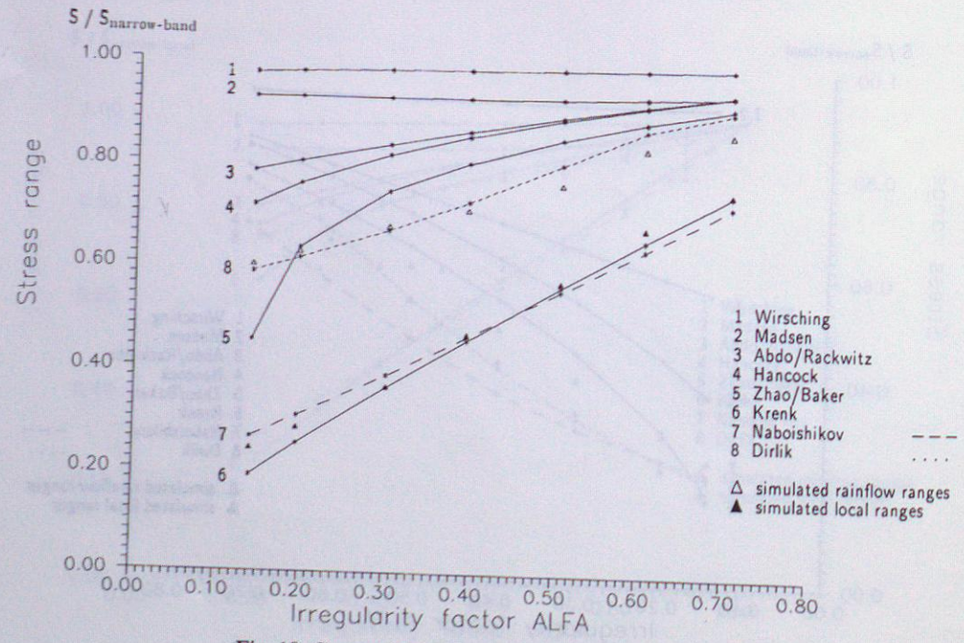

Fig. 18. Comparison for multimodal spectra ($m = 6$).

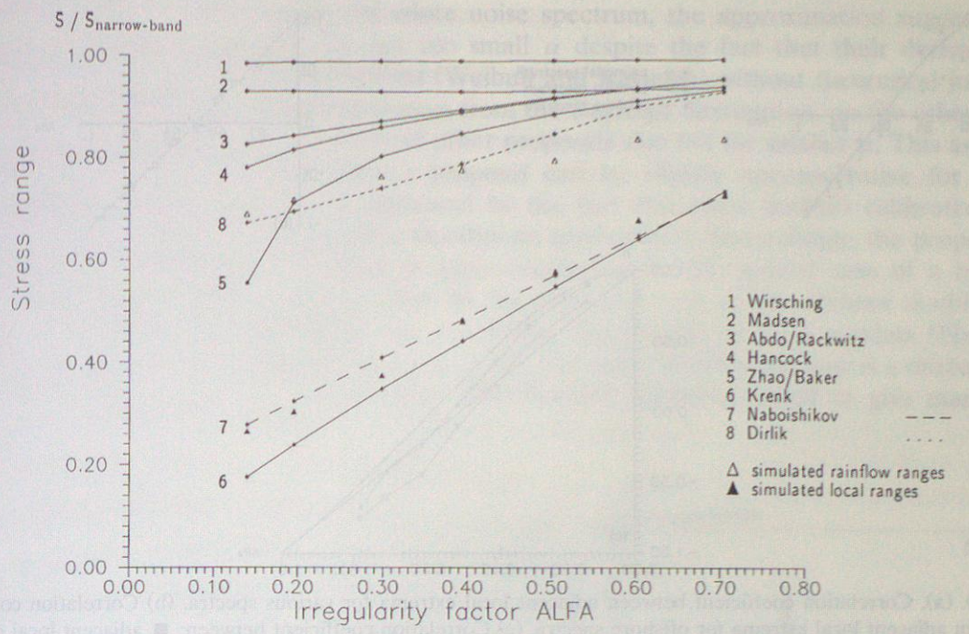

Fig. 19. Comparison for multimodal spectra ($m = 8$).

For each type of spectrum, a set of spectra with representative irregularity factors α were considered. The equivalent stress ranges were calculated for some of the most significant prediction models presented above. The ratios of equivalent ranges to the Miles damage indicators

$$\bar{S}_i/\bar{S}_{\text{narrow-band}} = \left(E\left[S_i^m\right]\right)^{1/m}/\bar{S}_{\text{Miles}} \tag{34}$$

are plotted as functions of α and for four different exponents $m = 2$, 4, 6 and 8 (see Figs. 8 to 19). The empirical rainflow and local ranges counted on the simulated stress time-histories generated from the considered spectra are reported, too. The equations due to Wirsching, Madsen, Kam/Dover (modified by Abdo/Rackwitz), Hancock Zhao/Baker, Krenk, Naboishikov and Dirlik were used in the comparative studies. For the bimodal spectra, Jiao/Moan's formula was included, too. The unimodal spectra are not considered because the range of their irregularity factor is limited to $\alpha \geqslant 0.745$.

4. Discussion

For $\alpha > 0.9$, all damage indicators yield fairly accurate results even for large m. As α tends to 1, they all converge to the narrow band result. The agreement between analytical approximations and the empirical estimates is always less satisfying as the parameter m grows. The theoretically most convincing and simplest formula in this region is probably formula (11) suggested by Krenk [13]. For $\alpha \leqslant 0.9$, the moments of local ranges and rainflow ranges already

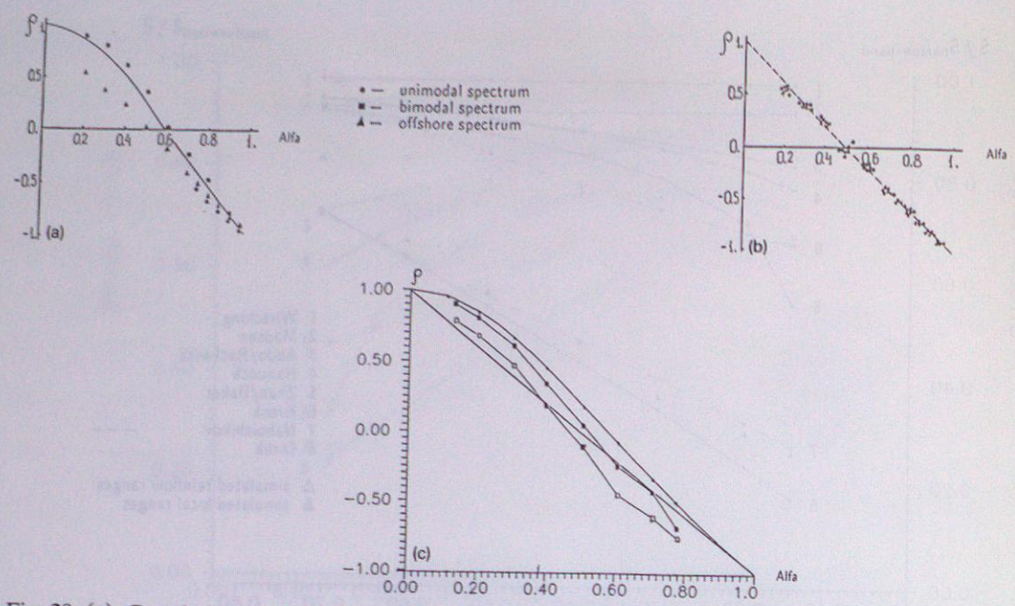

Fig. 20. (a). Correlation coefficient between adjacent local extrema for various spectra. (b) Correlation coefficient between adjacent local extrema for offshore spectra. (c) Correlation coefficient between: ■ adjacent local extrema; □ adjacent rainflow extrema; * model $\rho = (1-3\alpha^2)/(1+\alpha^2)$; · model $\rho = 1-2\alpha$, for multimodal spectra.

differ significantly. Therefore, local ranges and rainflow ranges must be discussed separately. The accuracy of the various models for $\alpha \leqslant 0.9$ depends essentially on the type of spectrum which was used for their calibration.

Naboishikov's model provides the best predictions to all of the simulated local range moments, whenever $\alpha \geqslant 0.6$. For exponents m higher than 2, Krenk's equation is equally satisfactory. However, these two proposals suffer from the shortcoming that they sometimes fail to provide conservative estimates. Furthermore, both equations strongly underestimate damage for really broad band stress spectra. The worst case occurs for the offshore double-peak spectrum. In Naboishikov's equation the underestimates are probably due to the approximation used for the correlation coefficient ρ between two adjacent local extrema. In fact, this parameter depends on the loading process which is not fully characterized by its irregularity factor α. The estimate $\rho_{i,i+1} \approx 1-2\alpha$ was derived from Fig. 20. In this figure the upper line represents the correlation coefficient estimated with $\rho_{i,i+1} = (1-3\alpha^2)/(1+\alpha^2)$. The local ranges follow a standard Rayleigh distribution (Madsen [30]) with parameters zero and $2\alpha^2$.

Wirsching's and Madsen's models do not properly reflect the dependence of the equivalent stress range on the irregularity factor α but are conservative with respect to rainflow and local range countings. For not too small α, the proposals by Ortiz/Chen and Larsen/Lutes can also be used. What is less satisfying with these models is that they retain the Rayleigh distribution for the ranges as a starting point for any value of the irregularity factor α. The derived correction factors also contain the parameter m. Additional information about the underlying spectrum in terms of spectral moments other than m_0, m_2 and m_4 is used. The indicates again that knowledge of m_0, m_2 and m_4 is not sufficient.

Apart from the case of a bimodal white noise spectrum, the approximation suggested by Zhao/Baker is also acceptable for not too small α despite the fact that their derivation is based on a mixture of range distributions (Weibull and Rayleigh) without theoretical justification. The deviation of the range distribution from the Rayleigh distribution, on the other hand, might just be the reason why a number of other proposals also fail for smaller α. This aspect is discussed further below. Zhao/Baker's proposal can be slightly unconservative for nearly narrow band process. This can be explained by the fact that these authors calibrated their model at rainflow ranges only occurring in offshore applications. Interestingly, the proposal by Jiao/Moan which from its derivation is quite convincing for the special case of a bimodal spectrum, is rather inaccurate for $\alpha \leqslant 0.6$. In the particular case of the offshore double-peak spectrum, the approaches based on the probability distribution of local maxima (Naboishikov/Kam/Dover, modified) are acceptable for $\alpha \geqslant 0.6$. The range distribution now is a mixture of a Gaussian and a Rayleigh-like distribution. The Hancock model is found to give not unsatisfactory

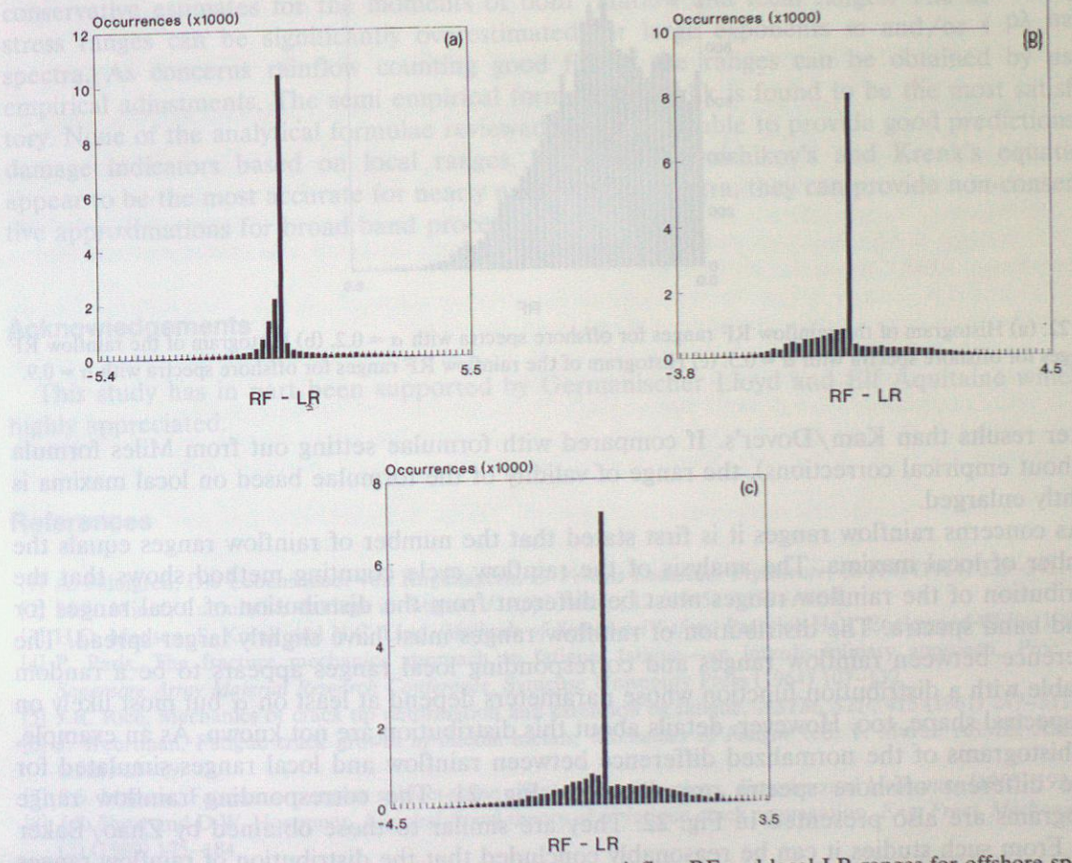

Fig. 21. (a). Histogram of the normalized difference between rainflow RF and local LR ranges for offshore spectra with $\alpha = 0.2$. (b) Histogram of the normalized difference between rainflow RF and local LR ranges for offshore spectra with $\alpha = 0.5$. (c) Histogram of the normalized difference between rainflow RF and local LR ranges for offshore spectra with $\alpha = 0.9$.

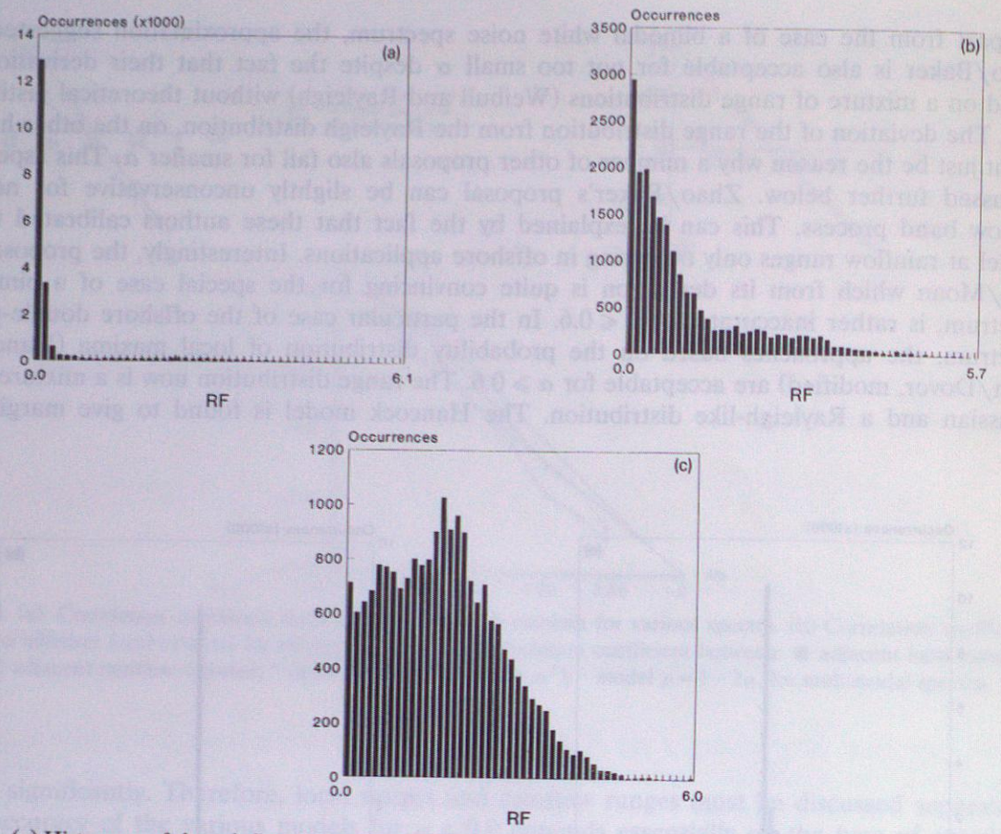

Fig. 22. (a) Histogram of the rainflow RF ranges for offshore spectra with $\alpha = 0.2$. (b) Histogram of the rainflow RF ranges for offshore spectra with $\alpha = 0.5$. (c) Histogram of the rainflow RF ranges for offshore spectra with $\alpha = 0.9$.

better results than Kam/Dover's. If compared with formulae setting out from Miles formula (without empirical corrections), the range of validity of the formulae based on local maxima is slightly enlarged.

As concerns rainflow ranges it is first stated that the number of rainflow ranges equals the number of local maxima. The analysis of the rainflow cycle counting method shows that the distribution of the rainflow ranges must be different from the distribution of local ranges for broad band spectra. The distribution of rainflow ranges must have slightly larger spread. The difference between rainflow ranges and corresponding local ranges appears to be a random variable with a distribution function whose parameters depend at least on α but most likely on the spectral shape, too. However, details about this distribution are not known. As an example, the histograms of the normalized difference between rainflow and local ranges simulated for three different offshore spectra are shown in Fig. 21. The corresponding rainflow range histograms are also presented in Fig. 22. They are similar to those obtained by Zhao/Baker [29]. From such studies it can be reasonably concluded that the distribution of rainflow ranges is a mixed distribution similar to eqn. (16), (30) or (32) but of a different type. In this sense Dirlik [28] took the right approach. This author even introduced a mixture of three distributions. From the above discussion a mixture of two distributions might have been sufficient.

Nevertheless, Dirlik's model appears to be the best over the full range of spectra, exponents m and irregularity factors α when measured against empirical rainflow ranges. This is not surprising since its theoretical formulation includes various empirical corrections and since it uses four spectral moments. Dirlik's predictions are also in good agreement with the numerical results for spectra including deterministic components. Therefore, this empirical formula can generally be recommended for practical use as a substitute for the exact rainflow cycle counting from measured or simulated stress/strain histories or to the somewhat complicated and laborious numerical integration approach proposed by Rychlik [9]. Note however that Dirlik's equation sometimes provides non-conservative estimates for small exponents m.

5. Conclusion

All available prediction models to bypass the cumbersome time history generation and cycle counting have a rather limited range of application. For arbitrary spectra, most of them provide conservative estimates for the moments of both rainflow and local ranges. The moments of stress ranges can be significantly overestimated for large exponents m and/or wide band spectra. As concerns rainflow counting good fits to the ranges can be obtained by using empirical adjustments. The semi empirical formula by Dirlik is found to be the most satisfactory. None of the analytical formulae reviewed above is capable to provide good predictions of damage indicators based on local ranges. Although Naboishikov's and Krenk's equations appear to be the most accurate for nearly narrow band spectra, they can provide non-conservative approximations for broad band processes.

Acknowledgements

This study has in part been supported by Germanischer Lloyd and Elf Aquitaine which is highly appreciated.

References

[1] A. Palmgren, Die Lebensdauer von Kugellagern, *Z. Vereins Deutscher Ingenieure*, 68 (14) (1924) 339–341.
[2] M.A. Miner, Cumulative damage in fatigue, *J. Appl. Mech.*, 12 (1945) A159–A164.
[3] H.O. Madsen, S. Krenk and N.C. Lind, *Methods of Structural Safety*, Prentice-Hall, Englewood-Cliffs, 1986.
[4] P. Paris, The fracture mechanics approach to fatigue, fatigue—an interdisciplinary approach, *Proc. 10th Sagamore Army Material Research Conference*, Syracuse University Press (1964) 107–132.
[5] J.R. Rice, Mechanics of crack tip deformation and extension by fatigue, *ASTM, STP*, 415 (1967) 247–311.
[6] J. Weertman, Fatigue crack growth in ductile metals, *Mechanics of Fatigue* (ed. T. Mura), ASME, AMD 47 (1981) 11–19.
[7] S.S. Manson, Fatigue: a complex subject-some simple approximations, *Experimental Mechanics* (1965) 193–226.
[8] J.S. Short and D.W. Hoeppner, A global/local theory of of fatigue crack propagation, *Eng. Fract. Mechanics*, 33 (2) (1989) 175–184.
[9] I. Rychlik, A new definition of the rain flow of cycle counting method, *Int. J. of Fatigue*, 9 (2) (1987) 119–121.
[10] I. Rychlik, Rain flow cycle distribution for a stationary Gaussian load process, Stat. Res. Rep. 86: 4, University of Lund, 1986, 1–36.
[11] J.W. Miles, On structural fatigue under random loading, *J. Aeronautical Sciences*, 21 (1954) 753–762.

[12] J.N. Yang, Statistics of random loading relevant to fatigue, *J. Engineering Mechanics*, 100 (3) (1974) 469–475.
[13] S. Krenk, A double envelope for stochastic processes, Report No. 134, Danish Center for Appl. Math. and Mech., 1978.
[14] S.R. Winterstein and C.A. Cornell, Fatigue and fracture under stochastic loading, *Proc. Fourth Int. Conf. on Structural Safety and Reliability*, 3 (1985) 745–749.
[15] J.R. Rice and F.P. Beer, On the distribution of rises and falls in a continuous random process, *Trans. ASME, J. Basic Engineering*, D-87-2 (1965) 398–404.
[16] G. Jiao and T. Moan, Probabilistic analysis of fatigue due to Gaussian load processes, *Probabilistic Eng. Mechanics*, 5 (2) (1990) 76–83.
[17] J.W. Hancock and D.S. Gall, Fatigue under narrow and broad stationary loading; J.W. Hancock and X.W. Huang, A reliability analysis of fatigue crack growth under random loading, Final Report of Cohesive Program of Research and Development into the Fatigue of Offshore Structure, (July 83–June 85), Marine Technology Directorate Ltd., 1985.
[18] J.M. Tunna, Fatigue life prediction for Gaussian random loads at the design stage, *Fatigue Fract. Eng. Mater. Struct.*, 9 (3) (1986) 169–184.
[19] J.C.P. Kam and W.D. Dover, Fast fatigue assessment procedure for offshore structures under random stress history, Proc. of the Institution of Civil Engineers, Part 2, 85 (1988) 689–700.
[20] S.T. Abdo and R. Rackwitz, Discussion to: J.C.P. Kam, W.D. Dover, Fast fatigue assessment procedure for offshore structures under random stress history, *Proc. of the Institution of Civil Engineers*, Part 2, 87 (1989) 645–649.
[21] M.R. Leadbetter, G. Lindgren and H. Rootzen, *Extremes and Related Properties of Random Sequences and Processes*, Springer, New York, 1983.
[22] S. Naboishikov, On the distribution of local extremes, ranges and means of Gaussian processes, *Proc. of the 4th IFIP WG 7.5 Conference*, Munich (1991) 305–312.
[23] P.H. Wirsching and M.C. Light, Fatigue under wide band random stresses, *Proc. of the ASCE, Journal of the Structural Division*, 106 (ST7) (1980) 1593–1607.
[24] P.H. Wirsching, Fatigue reliability for offshore structures, *J. Structural Engineering*, 110 (10) (1984) 2340–2356.
[25] P.H. Madsen, S. Frandsen, W.E. Hollay and J.C. Hansen, Dynamic analysis of wind turbine rotors for lifetime prediction, RISO Contract Report 102-43-51, 1983.
[26] K. Ortiz and N.K. Chen, Fatigue damage prediction for stationary wideband processes, *Proc. Fifth Int. Conf. on Application on Statistics and Probability in Soil and Struct. Eng.*, 1987.
[27] C.E. Larsen and L.D. Lutes, Predicting the fatigue life of offshore structures by the single-moment spectral method, *Probabilistic Eng. Mechanics*, 6 (2) (1991) 96–108.
[28] T. Dirlik, Application of computers in fatigue, Ph.D. Thesis, University of Warwick, 1985.
[29] W. Zhao and M.J. Baker, A new stress-range distribution model for fatigue analysis under wave loading, *Environmental Forces of Offshore Structures and their Prediction*, Kluwer Academic Publishers, 1990, pp. 271–291.
[30] H.O. Madsen, Deterministic and probabilistic models for damage accumulation, due to time varying loading, Dialog 5/82, Danish Engineering Academy, Civil Engineering Department, Denmark, 1982.
[31] J.N. Yang, Simulation of the random envelope processes, *J. Sound and Vibration*, 21 (1) (1972) 73–85.
[32] H. Daglas-Christiansen, Random number generators in several dimensions, Report Inst. for Mathematical Statistics & Operations Research (IMSOR). Technical University of Denmark, October 1975.

Appendix: simulation of Gaussian processes

The numerical modeling of Gaussian stress process realizations is carried out with four extremely different shapes of the spectral density

a) double-peak stress spectrum in joints of offshore structures (Fig. 1(a))

$$G(\omega) = \frac{\exp\left[-1050/(\omega T_D)^4\right]}{\omega^5 T_D^4 \left\{\left[1-(\omega/1.797)^2\right]^2 + (0.041\omega/1.797)^2\right\}}$$

b) bimodal white noise spectrum (Fig. 1(b))

$$G(\omega) = \begin{cases} A & \text{for } \omega_1 \leqslant \omega \leqslant \omega_2 \text{ and } \omega_3 \leqslant \omega \leqslant \omega_4; \\ 0 & \text{for other } \omega \end{cases}$$

c) clipped white noise (Fig. 1(c))

$$G(\omega) = \begin{cases} B & \text{for } \omega_1 \leqslant \omega \leqslant \omega_2; \\ 0 & \text{for other } \omega \end{cases}$$

d) multimodal spectrum (Fig. 1(d))

$$G(\omega) = G_Q(\omega) G_R(\omega)$$

with

$$G_Q(\omega) = \sum_{i=1}^{N_Q} \left[\frac{1}{2}\frac{\alpha_j K_j}{(\omega-\omega_j)^2+\alpha_j^2}\right] + \left[\frac{1}{2}\frac{\alpha_j K_j}{(\omega+\omega_j)^2+\alpha_j^2}\right]$$

and

$$G_R(\omega) = \sum_{i=1}^{N_R} \frac{C_i}{\left(\omega^2-\omega_i^2\right)^2 + \left(2\beta_i \omega \omega_i\right)^2}$$

where a_j and K_j are suitable load parameters and β_i is a damping ratio for some response transfer function. ω_i and ω_i are the corresponding modal frequencies. C_i is a parameter governing the energy output of the i-th mode.

For each spectrum a stress time-history $X(t)$ is generated by (Yang [31])

$$X(t) = \sum_{i=1}^{N} \left[2G(\omega_i)\Delta\omega_i\right]^{1/2} \cos(\omega_i + \phi_i)$$

where N is the number of frequency intervals, ϕ_i is the random phase and $\Delta\omega_i$ is the frequency interval. Up to $N = 1000$ frequency intervals are considered. Each extreme is found with an absolute precision of 10^{-5} with respect to the theoretical extreme. For each spectrum 40,000 extrema (minima and maxima) are generated. In order to avoid periodicities, the representative ω_i in each interval is calculated as

$$\omega_i = \sqrt{\frac{m_{4i}}{m_{2i}}}$$

where the spectral moments m_{2i} and m_{4i} correspond to the 2-nd and the 4-th spectral moments in the frequency interval $\Delta\omega_i$, respectively. Any periodicity of the simulated trajectory can be avoided in this way. In fact, even when ω_i is selected at random in the frequency interval $\Delta\omega_i$, periodicities can be observed. In order to determine exactly the size and location of the local extrema the derivative process is generated too.

A crucial issue when simulating the trajectories of random processes is the reliability of the random number generator. Several random number generators were subjected to extensive testing by the run-test (test for independence), a trend test and the Kolmogorov–Smirnov test (test for uniform distribution). The YRAN32 generator proposed by Dalgas-Christiansen [32] proved to be the best available producing almost ideal random numbers even for large sequences and all their segments.